ITM Web of Conferences **84**, 04023 (2026) https://doi.org/10.1051/itmconf/20268404023
ATCIDS 2026

Analysis of Underactuated Hand Exoskeletons with Elastic Structures

Juncheng Yang*

Mechanical and Electronic Control Engineering, Beijing Jiaotong University, Beijing, China

Abstract. Hand exoskeletons have broad application prospects in rehabilitation medicine, industrial assistance, and daily walking aids. Underactuated systems are popular due to their simple structure and low cost. However, existing designs lack adaptive ability when facing objects of different sizes and lack an effective mechanism to realize autonomous adjustment of grasping posture and force. The kinematics model is established and simulated by the vector closed-loop method. The static model is established based on Hooke's law. The relationship between the grasping force and the spring deformation is derived, and the target grasping force of 10N is set. The results show that the metacarpophalangeal joint (MCP) Angle is stable in the safe range of -65° to 4°, and the structure can autonomously adjust the grasping posture and force distribution to improve adaptability. The results show that the structure can automatically adjust the grasping posture and force distribution according to the characteristics of the object, and effectively improve the grasping stability and adaptability. This design provides a feasible technical path for the intelligence and practicability of the underactuated hand exoskeleton

1 Introduction

As a key research object in the field of human-computer interaction, the hand exoskeleton has demonstrated significant application potential in various fields. In terms of rehabilitation medical treatment, it can assist patients in hand function rehabilitation training, help patients restore hand motor ability, and improve the level of self-care [1][2]. In industrial operation scenarios, it can enhance workers' hand strength and operation accuracy, improve work efficiency, and reduce labor intensity [3]. In the field of daily living assistance, it can provide practical help for people with mobility problems, making it easier for them to complete daily activities [4].

Underactuated hand exoskeletons have attracted much attention due to their unique advantages. Compared with the fully actuated hand exoskeleton, the underactuated hand exoskeleton has the remarkable characteristics of simple structure, low cost, and relatively simple control. E. Chowdhury et al. proposed a 3-DOF underactuated finger exoskeleton for rehabilitation. The parameters of the chain length were optimized for the 3-DOF exoskeleton model, and the variable ranges of the metacarpophalangeal joint and the end-

*Corresponding author's email: 23222055@bjtu.edu.cn

phalangeal joint were obtained as [90cm,140cm] and [25cm,35cm], respectively, to adapt to the size range of the finger [5]. Amirpour described a new type, such as the underactuated, connecting rod drive mechanism of the exoskeleton and kinematics optimization, which puts forward an optimized exoskeleton long chain algorithm to maximize exoskeleton working space and the tactile feedback in the HEXON [6]. Akinniyi etc. put forward a kind of promote the exoskeleton device of finger and repeatedly take the initiative to training involves flexion and extension, using serial components and adaptive mechanism slide flexible spring (elastic modulus of 193 gpa) and three pieces of rigid parts, can produce 100 n largest hand grasp grip strength [7]; CAI et al. designed an exoskeleton for piano teaching underactuated manipulator exoskeleton, which realized the coupling movement of distal finger DIP, proximal finger PIP and metacarpophalangeal MCP [8].

However, the current underactuated hand exoskeleton generally has the problem of insufficient adaptability when grasping objects of different sizes [9]. In practice, the size, shape, and material of objects differ in thousands of ways. Traditional underactuated hand exoskeletons are hard to use without complex adjustments, resulting in inefficient and unstable grasping of objects, which greatly limits their application range and performance.

In this paper, the structure of the underactuated hand exoskeleton is improved, and the traditional rigid link is replaced by a multi-spring combination, aiming to improve its adaptive grasping ability for objects of different sizes.

2 Improved structure design of the underactuated hand exoskeleton

The traditional underactuated hand exoskeleton usually adopts a link-joint structure design. Its basic components include multiple finger modules, and each finger module is composed of several links connected by joints. These joints generally have one or a limited number of degrees of freedom and realize cooperative movement through specific transmission mechanisms. From the Angle of kinematics, due to the relatively few degrees of freedom, the trajectory and attitude adjustment ability are limited. In grasping objects, finger movements are mainly for easy opening and closing action; it is difficult to accurately join the surface of objects of different shapes and sizes. Due to the poor controllability and flexibility of finger movements, it is often difficult to achieve ideal grasping effects for complex objects.

In order to solve the above problems of the traditional underactuated hand exoskeleton, this paper proposes an improved design concept based on a spring combination. The introduction of spring aims to make use of the elastic deformation characteristics of the spring, so that the hand exoskeleton can automatically adjust its grasping posture and grasping force according to the shape, size, and hardness of the object during the grasping process. As a common elastic element, a spring has good elasticity and adjustability, which can generate corresponding deformation under different external forces, thus providing variable forces and displacements for the hand exoskeleton and enhancing its adaptability to different objects (Fig. 1).

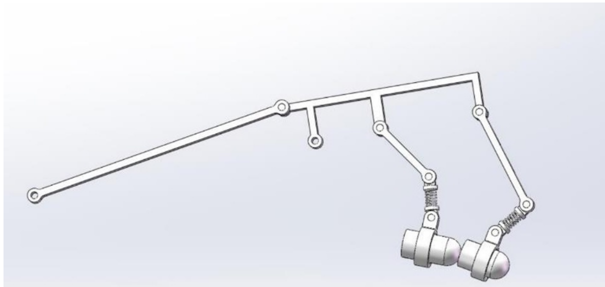

Fig. 1. Elastic underactuated hand exoskeleton model (Photo/Picture credit: Original).

When the hand exoskeleton comes into contact with an object, the reaction force exerted by the object on the hand exoskeleton deforms the spring. Depending on the shape and size of the object, different springs will deform in response to different forces. For example, for smaller and softer objects, springs with smaller elastic coefficients will deform more first to fit the surface of the object and provide gentle grasping forces; While for a larger and harder object, the spring with a larger elastic coefficient will deform appropriately under the action of a larger force, ensuring that enough grasping force is provided to stably grasp the object. Through the deformation of the spring, the hand exoskeleton can automatically adjust its grasping posture and grasping force to realize the adaptive grasping of objects of different sizes.

3 Kinematic analysis

In order to deeply study the motion characteristics of the improved underactuated hand exoskeleton, this section establishes the corresponding kinematic model based on its mechanical structure. This model aims to reveal the mapping relationship between actuation input (such as actuator stroke) and finger joint output angles (MCP, PIP), thereby laying a theoretical foundation for subsequent static analysis and performance optimization.

In this paper, the Vector Closed-Loop Method is used to construct the kinematic model. This method establishes a series of vector equations by analyzing the closed geometric loop of each link in the mechanism, and then solves the Angle parameters of the key joints.

3.1 Simplification of the mechanism and establishment of the coordinate system

Firstly, the mechanism of a single finger (take the index finger as an example) is simplified. Each finger component is regarded as a rigid link, and the link mass and joint friction are ignored. A two-dimensional plane coordinate system was established, and the origin was located at the intersection of the support platform on the back of the hand and the middleware (Figs. 2 and 3).

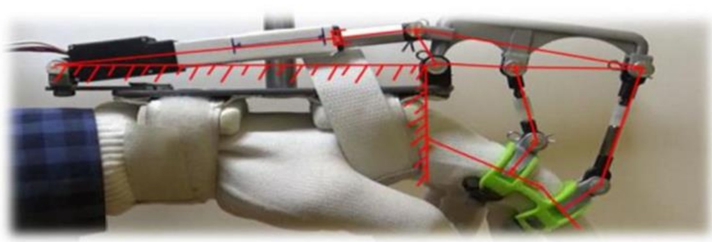

Fig. 2. Traditional RobHand conFiguration with a single finger [10]

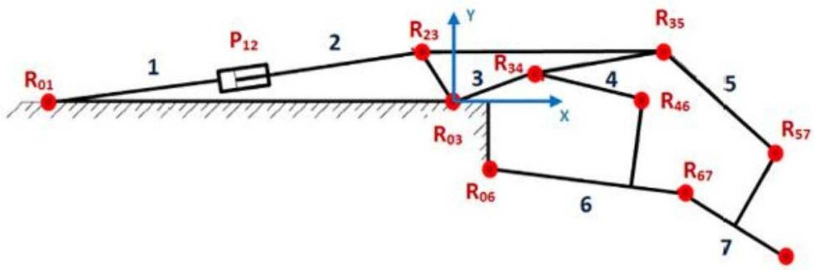

Fig. 3. Joint node diagram [10]

The main geometric parameters are defined as follows (Fig. 4):

L_2, L_3 is the spacing between the center of the MCP joint and the origin of the coordinates in the direction x and y. L_4 is the distance between MCP joint and PIP joint. L_8 is the distance between PIP joint and DIP joint.L_6 L_{10} is the length of the spring connected to the metacarpophalangeal joint and proximal phalangeal joint.

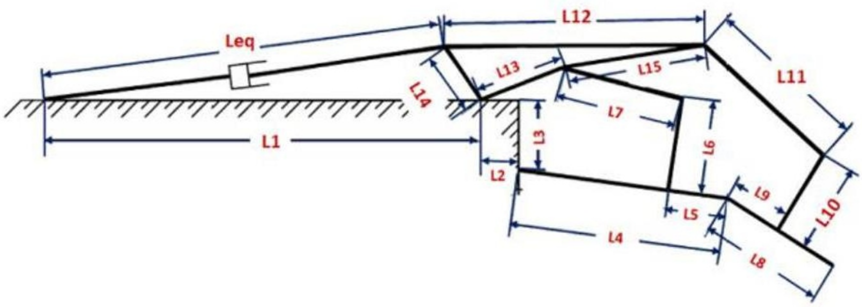

Fig. 4. Length parameter map [10]

The main Angle parameters are defined as follows (Fig. 5):

The Angle α is the MCP (metacarpophalangeal) joint Angle, with positive values indicating extension and negative values indicating flexion. The Angle β is the PIP (proximal knuckles) joint Angle, with positive values indicating extension and negative values indicating flexion. The Angle φ is the Angle of the middleware with respect to the coordinate system.

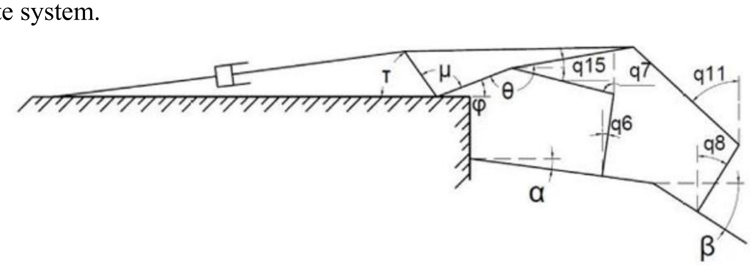

Fig. 5. Angle parameter plot [10]

3.2 Closed-loop equation derivation

According to the topological structure of the mechanism, two key closed loops can be identified.

Closed loop one (Fig. 6): Used to solve the MCP joint angles α . Its vector equation is as follows.

$\vec{l}_2 + \vec{l}_3 + \vec{l}_4 - \vec{l}_5 + \vec{l}_6 + \vec{l}_7 + \vec{l}_{13} = 0(1)$

Decomposing the above vector equation to the X-axis and Y-axis, it obtains:

$X\ axis: \vec{l}_2 + (\vec{l}_4 - \vec{l}_5)\cos\alpha + \vec{l}_6 \sin q_6 - \vec{l}_7 \sin q_7 - \vec{l}_{13}\cos\varphi = 0(2)$

$Y\ axis: \vec{l}_3 + (\vec{l}_4 - \vec{l}_5)\sin\alpha - \vec{l}_6 \cos q_6 - \vec{l}_7 \cos q_7 + \vec{l}_{13}\sin\varphi = 0(3)$

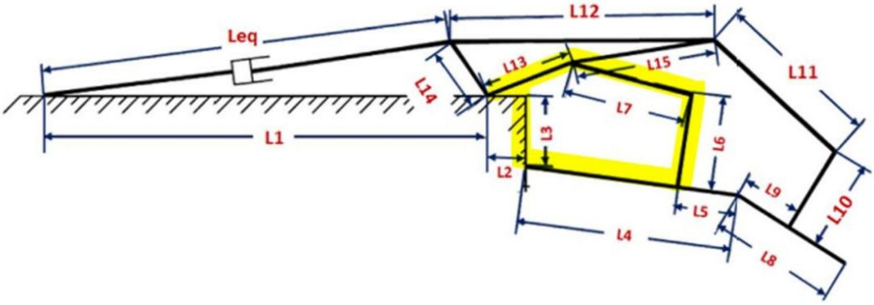

Fig. 6. Closed-loop model of the metacarpophalangeal joint (Photo/Picture credit: Original).

It can be obtained from Fig. 5 that α=q_6, considering that although the spring will also be offset in the axial direction by the tangential force (Fig. 7) when it generates the elastic force, the Angle is very small and can be ignored, so the Angle relationship still holds.

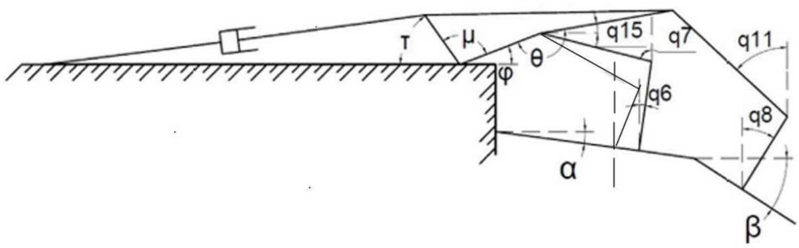

Fig. 7. Angle relation after spring offset (Photo/Picture credit: Original).

Closed Loop II (Fig. 8): Used to solve the PIP joint Angle. βIts vector equation is:

$\vec{l}_2 + \vec{l}_3 + \vec{l}_4 + \vec{l}_9 + \vec{l}_{10} + \vec{l}_{11} + \vec{l}_{15} + \vec{l}_{13} = 0(4)$

Decomposing it to the X-axis and Y-axis, it obtains:

$X\ axis: \vec{l}_2 + \vec{l}_4\cos\alpha + \vec{l}_9\cos\beta + \vec{l}_{10}\sin q_8 - \vec{l}_{11}\sin q_{11} - \vec{l}_{15}\cos q_{15} - \vec{l}_{13}\cos\varphi =$
$0(5)$

$Y\ axis: \vec{l}_3 + \vec{l}_4\sin\alpha + \vec{l}_9\sin\beta - \vec{l}_{10}\cos q_8 - \vec{l}_{11}\cos q_{11} + \vec{l}_{15}\sin q_{15} + \vec{l}_{13}\sin\varphi = 0(6)$

Similarly, it follows from Fig. 5 that α=q_7

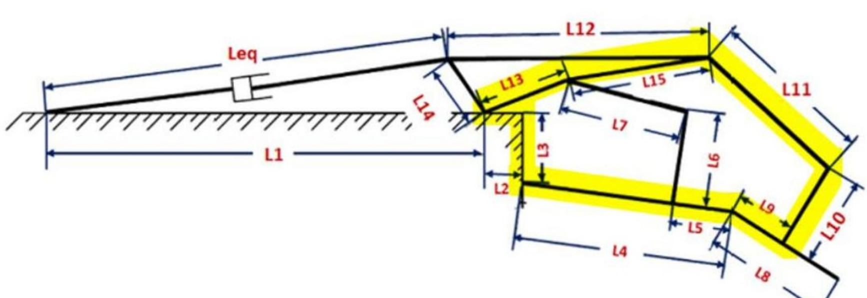

Fig. 8. Closed-loop model of the metacarpophalangeal and proximal knuckle joints (Photo/Picture credit: Original).

3.3 Calculation of key parameters

According to the geometric relationship, the position of DIP joint and PIP joint is

$$\begin{cases} PIP_X = \vec{l}_2 + \vec{l}_4 \cos\alpha \\ PIP_Y = -\vec{l}_3 + \vec{l}_4 \sin\alpha \\ DIP_X = \vec{l}_2 + \vec{l}_4 \cos\alpha + \vec{l}_8 \cos\beta \\ DIP_Y = -\vec{l}_3 + \vec{l}_4 \sin\alpha + \vec{l}_8 \sin\beta \end{cases} \quad (7)$$

Considering the linear and angular parameters of RobHand, the MCP and PIP joint angles of each finger are a function of the linear actuator elongation, so they must first be calculated as shown in the equation τ.

$$\tau = \arccos\left(\frac{l_{14}^2 + l_1^2 - L_{eq}^2}{2 l_{14} l_1}\right)(8)$$

μ Is determined by the geometry of the middleware, so it is constant and known. Hence the calculation is as follows $\varphi = \pi - \mu - \tau(9)$

3.4 Kinematic model simulation

According to the kinematics model simulation in MATLAB, the following image (Fig. 9) can be obtained. It can be seen that the change of mcp joint Angle is relatively stable, and there is no mutation. In addition, the change of mcp joint Angle is about 4 degrees to -65 degrees, which belongs to the safe interval of this joint, indicating that users can have a more comfortable use experience under this conFiguration. It shows that users can have a more comfortable use experience under this conFiguration, and it will not cause damage to the joint.

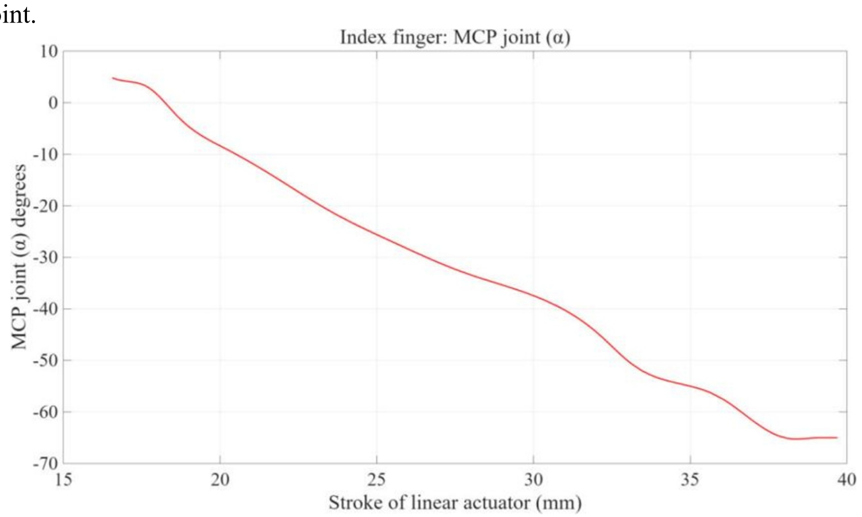

Fig. 9. Curve of the MCP joint with actuator displacement (Photo/Picture credit: Original).

On this basis, considering that the spring connected to the finger end will produce compression deformation under force extrusion, the $l_6$and l_{10}will gradually decrease in the kinematic model, so it discusses the limit case when the$l_6$and l_{10} is reduced to 0, and the equation changes as follows:

$X\ axis: \vec{l}_2 + (\vec{l}_4 - \vec{l}_5)\cos\alpha - \vec{l}_7 \sin q_7 - \vec{l}_{13} \cos\varphi = 0(10)$

$Y\ axis: \vec{l}_3 + (\vec{l}_4 - \vec{l}_5)\sin\alpha - \vec{l}_7 \cos q_7 + \vec{l}_{13} \sin\varphi = 0(11)$

Through MATLAB simulation, the following image (Fig. 10) is obtained:

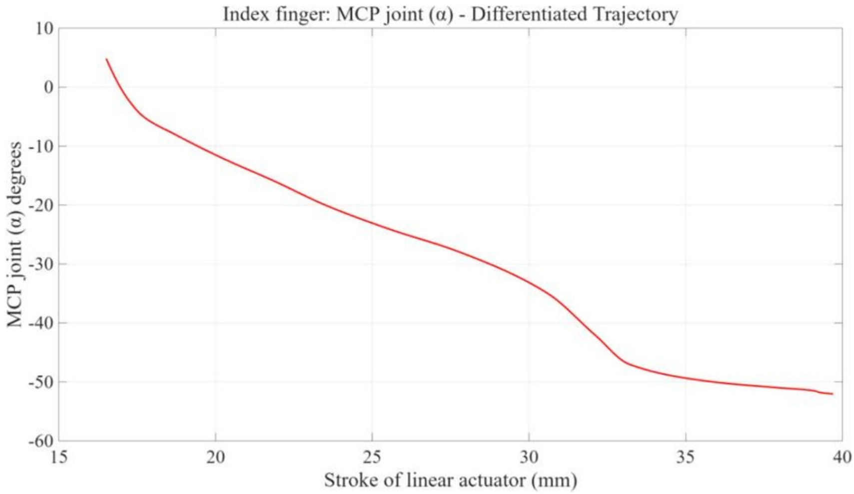

Fig. 10. MCP joint Angle curve under complete spring compression (Photo/Picture credit: Original).

It can be seen that the image trend does not change greatly and is more stable. In addition, the final Angle of the MCP joint is reduced to about 52 degrees, which indicates that no matter whether the user is in the action of grasping the object or not, the spring does not affect safety and comfort, but only affects the initial and final angles.

4 Discussion

Although the underactuated hand exoskeleton based on a spring combination shows the potential of adaptive grasping in static simulation, there are still several key problems to be solved in practical application. Among them, the dynamic change and accurate control of grasping force are the core shortcomings of current research. Firstly, the existing models only analyze the force transmission based on static assumptions, while the motion inertia of the object, the elastic lag effect of the spring, and the fluctuation of the driving speed in the actual grasping process will lead to the instantaneous peak force and energy dissipation. These dynamic factors directly affect the grasping stability and user safety, but they have not been verified by experiments [11]. Secondly, the nonlinear behavior of the spring (such as stiffness attenuation caused by material fatigue) will reduce the accuracy of force output in long-term use, and the influence of individual hand size and muscle strength differences on force adaptation also lacks ergonomic data support. In addition, the force can not be adjusted in real time according to the material and shape of the object in the open-loop control mode, which makes the system difficult to cope with the grasping requirements of fragile or irregular objects. The essence of these problems points to the lack of dynamic force modeling and closed-loop control capabilities, and it is necessary to break through the bottleneck through experiments and algorithm optimization.

Future research will focus on the combination of 3D printing and lightweight aluminum alloy processing to manufacture single finger and full hand exoskeleton prototypes with multi-spring structure, integrating micro servo motors and flexible transmission cables. The force measurement table and optical motion capture system are used to measure the grasping force distribution, joint Angle change and energy efficiency under different object sizes in the laboratory environment, and the results are compared with the simulation results. The sensor data acquisition and control algorithm are deployed based on the embedded platform, and the active object recognition and adaptive grasping experiments are carried out to further verify the reliability of the simulation structure.

5 Conclusion

Aiming at the problem of insufficient adaptability of traditional underactuated hand exoskeleton when grasping objects of different sizes, this paper proposes a structure improvement scheme based on multi-spring combination. By replacing the rigid link with a deformable spring element, the exoskeleton is endowed with passive adaptive ability, which can automatically adjust the grasping posture and force distribution according to the size and hardness of the object. The kinematic analysis shows that the improved structure has a stable mapping relationship between the drive input and the joint Angle, and the motion range of the MCP joint is reasonable (about -65° to 4°), and it is still in the safe range under the limit of complete compression of the spring, which ensures the comfort and safety of the wearer. The static modeling and optimization further determined the optimal value range of the spring elastic coefficient. Under the premise of meeting the joint torque safety and spring deformation constraints, the stable output of the target grasping force (such as 10N) was achieved. The simulation results verify the effectiveness of the proposed design in terms of force transfer efficiency and adaptive grasping, which significantly improves the compatibility with the diversity of external objects. However, there are still some limitations in this study: the current model is based on idealized assumptions, ignoring friction, spring nonlinear characteristics, and inertial effects in dynamic grasping process. Moreover, the experimental part has not been tested by a physical prototype, and the verification of actual grasping data is lacking. Future work will focus on the prototype operation and grasping performance test in real scenes, and introduce sensor feedback to realize closed-loop control, so as to further improve the robustness and intelligence of the system.

References

1. M. Sarac, M. Solazzi, and A. Frisoli, Design requirements of generic hand exoskeletons and survey of hand exoskeletons for rehabilitation, assistive, or haptic use. IEEE Trans. Haptics **12**(4), 400–413 (2019)
2. Y. Zhang, Z. Song, and R. Fu, Hand exoskeleton for rehabilitation using a flexible screw mechanism. In Proc. IEEE Int. Conf. Robot. Biomimetics (ROBIO), pp. 1–6 (2023)
3. T. Guo, Z. Zhou, Y. Jin, et al., New wearable auxiliary artificial picking pineapple device design. J. Mech. Des. (5), 16–21 (2025)
4. K. Minamii and M. Yoshikawa, A hand exoskeleton with 3D-printed compliant mechanisms to assist grasping. In Proc. IEEE Eng. Med. Biol. Soc. (EMBC), pp. 1–4 (2024)
5. E. Chowdhury, S. Bamoriya, P. Kaushik, C. S. Kumar, and M. Mahadevappa, Design and optimization study of a linkage-driven finger of a hand exoskeleton for use in post-stroke rehabilitation. In Proc. IEEE Eng. Med. Biol. Soc. (EMBC), pp. 1–6 (2025)
6. E. Amirpour, Design and optimization of a multi-DOF hand exoskeleton for haptic applications. In Proc. Int. Conf. Robot. Mechatronics (ICRoM), pp. 270–275 (2019)
7. O. T. Akinniyi, A low-cost orthosis using a compliant spring mechanism for post-stroke hand rehabilitation. In Proc. IEEE Niger. Int. Conf. Disruptive Technol. Sustain. Dev. (NIGERCON), pp. 1–4 (2022)
8. R. Cai, B. Ding, Z. Li, et al., Touch-the-piano-keys action-based education assistive exoskeleton manipulator design. Control Decis. **37**(2), 314–322 (2022)

9. D. Huamanchahua, P. Toledo-Garcia, J. Aguirre, and S. Huacre, Hand exoskeletons for rehabilitation: A systematic review. In Proc. IEEE Int. IoT Electron. Mechatronics Conf. (IEMTRONICS), pp. 1–6 (2022)
10. V. Moreno-SanJuan, A. Cisnal, J.-C. Fraile, J. Perez-Turiel, and E. de-la-Fuente, Design and characterization of a lightweight underactuated RACA hand exoskeleton for neurorehabilitation. Robot. Auton. Syst. **143**, 103828 (2021)
11. H. Li, Design of an assistive hand exoskeleton based on the principles of the human hand grasp. In Proc. Int. Conf. Mechatronics Mach. Vis. Pract. (M2VIP), pp. 1–6 (2023)